

Mean-field model of the ferromagnetic ordering in the superconducting phase of $\text{ErNi}_2\text{B}_2\text{C}$

Jens Jensen

Ørsted Laboratory, Niels Bohr Institute fAPG, Universitetsparken 5, DK-2100 Copenhagen, Denmark

(Received 9 January 2002; published 4 April 2002)

A mean-field model explaining most of the details in the magnetic phase diagram of $\text{ErNi}_2\text{B}_2\text{C}$ is presented. The low-temperature magnetic properties are found to be dominated by the appearance of long-period commensurate structures. The stable structure at low temperatures and zero field is found to have a period of 40 layers along the a direction, and upon cooling it undergoes a first-order transition at $T_C \approx 2.3$ K to a different 40-layered structure having a net ferromagnetic component of about $0.4\mu_B/\text{Er}$. The neutron-diffraction patterns predicted by the two 40-layered structures, above and below T_C , are in agreement with the observations of Choi *et al.* [Phys. Rev. Lett. **87**, 107001 (2001)].

DOI: 10.1103/PhysRevB.65.140514

PACS number(s): 74.70.Dd, 75.25.+z, 75.10.Jm

A number of the $(\text{R})\text{Ni}_2\text{B}_2\text{C}$ compounds are normal s -type superconductors with a T_C of the order of 10 K. The superconductors are all of type II with a κ in the range of 6–12. They are magnetic due to the rare-earth ions and in four of the compounds ($R = \text{Dy}, \text{Ho}, \text{Er}, \text{or Tm}$) the rare-earth ions are antiferromagnetically ordered in the superconducting phase.¹ The ordering wave vector \mathbf{Q} in Er borocarbide is along an a axis and has a length of about 0.55 (in units of $2\pi/a$), and the ordered moments are along the $a(b)$ axis perpendicular to \mathbf{Q} ; the Néel temperature is $T_N = 6$ K and $T_C = 11$ K. The rare-earth ions are placed in a body-centered tetragonal lattice, and in the case of Er $a = b = 3.502$ Å and $c = 10.558$ Å. It was proposed already in 1996 that the Er ions in $\text{ErNi}_2\text{B}_2\text{C}$ develop a small ferromagnetic component in addition to the antiferromagnetic one below 2.3 K.² This makes the Er compound particularly interesting as presenting the case of a weak ferromagnetic state existing well below H_{c2} . The ferromagnetic moment at 2 K was estimated to be $0.33\mu_B$ per Er ion creating an internal magnetic field $4\pi M \approx 0.60$ kOe close to the estimated value of the lower critical field H_{c1} . Kawano *et al.*³ did detect a ferromagnetic moment below 2.3 K in a neutron-diffraction experiment, but saw no sign of a spontaneous vortex phase. Recently, Choi *et al.*⁴ have made a detailed neutron-diffraction experiment in which they measured all the higher harmonics of the antiferromagnetic structures occurring just above and below the Curie temperature, and they concluded that the structure at 1.3 K has a ferromagnetic component of about $0.57\mu_B$ per Er ion. Kawano-Furukawa *et al.*⁵ have performed the same experiments as Choi *et al.* and obtained similar results for the scattering cross section.

It is known that the superzone energy gaps on the Fermi surface induced by the antiferromagnetic ordering may have a strong effect on the superconducting order parameter.^{6,7} On the other hand, the superconducting order parameter does not seem to affect the antiferromagnetic ordering, but is of importance for a ferromagnetic system at low fields. The Anderson-Suhl effect,⁸ that the Ruderman-Kittel-Kasuya-Yoshida (RKKY) of the rare-earth ions is strongly reduced in the long wavelength limit, has been demonstrated⁷ to be important in $\text{TmNi}_2\text{B}_2\text{C}$. Here, I shall mostly concentrate on understanding the behavior of the magnetic moments in

$\text{ErNi}_2\text{B}_2\text{C}$, and to start with I neglect the influence of the superconducting ordering on the magnetic properties.

The crystal-field parameters of the Er ions have been determined by Gasser *et al.* from the crystal-field transitions observed by neutron scattering and from the high-temperature susceptibility data.⁹ These parameters are used in the present work except that B_2^0 has been scaled by a small factor (1.08), see Table I. The ground state is a doublet, and an excited doublet is lying only about 0.6–0.7 meV above the ground state. This configuration leads to a four-clock behavior of the moments at low temperatures, i.e., the Er ions are easily magnetized along $\langle 100 \rangle$, they are hard to magnetize along the c direction, and when the field is applied along $\langle 110 \rangle$ the moments are approximately a factor $\sqrt{2}$ smaller than the moments in the $\langle 100 \rangle$ case.

Detlefs *et al.* have observed that the antiferromagnetic ordering in $\text{ErNi}_2\text{B}_2\text{C}$ is accompanied by an orthorhombic distortion of the lattice, so that $a/b - 1 = \epsilon_{11} - \epsilon_{22} \approx 2 \times 10^{-3}$ at 3.7 K.¹⁰ Because of this observation, the following quadrupole coupling is included in the model:

$$\mathcal{H}_{\text{me}} = - \sum_i \sum_{m=\pm 2} K_\gamma^m [O_2^m(i) \langle O_2^m \rangle - \frac{1}{2} \langle O_2^m \rangle^2]. \quad (1)$$

The definition of the Stevens operators may be found in Ref. 11. $\langle O_2^m \rangle$ is the expectation value of the operator averaged over all ions. The contribution to the free energy of the modulated quadrupolar moments (at the wave vector $2\mathbf{Q}$) is a factor of 100 smaller than that of the uniform term and is neglected. The value of K_γ^{-2} is undetermined, but is only of minute importance for the model and is assumed to be equal K_γ^2 . The calculated value of $\langle O_2^2 \rangle$ is 34.6 at 3.7 K. Assuming $(c_{11} - c_{12})/2$ to be about 5×10^{11} ergs/cm³ (consistent with a Debye temperature of the order of 400 K) then the distortion observed by Detlefs *et al.* indicates a value of $K_\gamma^2 = (1/2N)(c_{11} - c_{12})[(\epsilon_{11} - \epsilon_{22})/\langle O_2^2 \rangle]^2 \approx 0.7 \times 10^{-4}$ meV.

TABLE I. The Stevens operator parameters (meV).

B_2^0	B_4^0	B_4^4	B_6^0	B_6^4
−0.0173	0.147×10^{-3}	-3.3×10^{-3}	-0.122×10^{-5}	2.16×10^{-5}

TABLE II. The planar two-ion coupling parameters (μeV).

n	0	1	2	3	4	5	6	9	LD
$\mathcal{J}_\perp(n)$	5.847	-3.816	-4.786	-0.650	1.500	-1.500		0.29	0.29
$\mathcal{J}_\parallel(n) - \mathcal{J}_\perp(n)$	-14.286	-3.024	3.106	-0.630	0.250	-0.084	0.030		

This value is close to the one used in the final fit: $K_\gamma^2 = K_\gamma^{-2} = 0.8 \times 10^{-4} \text{ meV}$. The magnetoelastic coupling is not essential for the model, but it improves clearly the fits to the magnetization curves discussed below.

The two-ion interaction is assumed to be the sum of a Heisenberg interaction and the classical dipole-dipole interaction:

$$\mathcal{H}_{JJ} = -\frac{1}{2} \sum_{i,j} \mathcal{J}(ij) \mathbf{J}_i \cdot \mathbf{J}_j - \frac{1}{2} \sum_{i,j} \mathcal{J}_D D_{\alpha\beta}(ij) J_{i\alpha} J_{j\beta} \quad (2)$$

with $\mathcal{J}_D = N(g\mu_B)^2 = 1.194 \text{ } \mu\text{eV}$ and

$$D_{\alpha\beta}(ij) = \frac{3(r_{i\alpha} - r_{j\alpha})(r_{i\beta} - r_{j\beta}) - |\mathbf{r}_i - \mathbf{r}_j|^2 \delta_{\alpha\beta}}{N|\mathbf{r}_i - \mathbf{r}_j|^5}. \quad (3)$$

The two-ion Hamiltonian is accounted for in the mean-field approximation, $\mathbf{J}_i \cdot \mathbf{J}_j \approx \mathbf{J}_i \cdot \langle \mathbf{J}_j \rangle + \langle \mathbf{J}_i \rangle \cdot \mathbf{J}_j - \langle \mathbf{J}_i \rangle \cdot \langle \mathbf{J}_j \rangle$. All the ordered structures are described by a wave vector \mathbf{Q} along the a axis and consist of ferromagnetic sheets perpendicular to \mathbf{Q} . This means, first, that the different positions of the ions in the two sublattices have no direct consequences, corresponding to the use of a double-zone representation along $\langle 100 \rangle$, and, second, that only the total couplings between the different ferromagnetic layers are important in the model. The interplanar coupling parameters are

$$\mathcal{J}_{\parallel,\perp}(n) = \sum_{\mathbf{r}_j \cdot \mathbf{a} = na^{2/2}} [\mathcal{J}(0j) + \mathcal{J}_D D_{\parallel,\perp}(0j)] \quad (4)$$

and the corresponding Fourier transforms $\mathcal{J}_{\parallel,\perp}(\mathbf{q})$. The parameter $\mathcal{J}_\perp(\mathbf{q})$ is the coupling between the components of the moments within the a - b plane perpendicular to \mathbf{q} .

The final values of the coupling parameters are given in Table II, where $\mathcal{J}_\perp(n)$ have been derived from the fitting of the experimental results and $\mathcal{J}_\parallel(n) - \mathcal{J}_\perp(n)$ have been calculated using Eq. (3). The analysis indicates that $\mathcal{J}_\perp(\mathbf{q})$ is strongly peaked at $\mathbf{q} \approx \mathbf{Q}$. In order to create such a peak I have introduced the long-distance coupling parameter $\mathcal{J}_\perp(\text{LD})$, in terms of which

$$\mathcal{J}_\perp(n) = \mathcal{J}_\perp(\text{LD}) \cos(0.558n\pi); \quad n = 10, 11, \dots, 16.$$

The remaining couplings for $n = 0, 1, \dots, 5$, and 9 have been considered individually as independent fitting parameters. The results for $\mathcal{J}_\perp(\mathbf{q})$ and $\mathcal{J}_\parallel(\mathbf{q})$ are shown in Fig. 1. The most important model parameters are the wave vector at which $\mathcal{J}_\perp(\mathbf{q})$ has its maximum, at $\mathbf{Q}_0 = 0.558 \mathbf{a}^*$, the maximum value itself $\mathcal{J}_\perp(\mathbf{Q}_0)$ and $\mathcal{J}_\perp(\mathbf{0}) = \mathcal{J}_\parallel(\mathbf{0}) = -12 \text{ } \mu\text{eV}$. The latter value is determined from the high-field magnetization, and the parameter $\mathcal{J}_\perp(\mathbf{Q}_0)$ is assumed fixed at $21.56 \text{ } \mu\text{eV}$, which leads to a mean-field value of $T_N = 6.0 \text{ K}$. The classical interaction gives rise to a large nega-

tive difference $\mathcal{J}_\parallel(\mathbf{q}) - \mathcal{J}_\perp(\mathbf{q})$ of the same order of magnitude as the Heisenberg term itself, and it favors strongly the transverse polarization of the oscillating ordered moments. Due to the singular behavior of the dipole sum the difference is cancelled at zero wave vector, i.e., $\mathcal{J}_\parallel(\mathbf{q})$ makes a jump by $4\pi\mathcal{J}_D = 15.0 \text{ } \mu\text{eV}$ in the limit of $\mathbf{q} \rightarrow \mathbf{0}$.

The neutron-diffraction experiment of Choi *et al.*⁴ revealed a large third harmonic below $T_N/2$. This shows that the modulation of the ordered moments approaches a square wave, and thereby that commensurate structures become stabilized. The commensurate structures appearing may be rather complex limiting the possibility of deciphering the neutron-diffraction experiments. It has previously turned out to be of great value to assist the analysis of diffraction experiments by theoretical model calculations of the stability of the structures which may occur. This has been the case in the study of the long-period commensurate structures in the elemental erbium and holmium metals.¹¹⁻¹³ The method used here is the same as in the previous works, i.e., the free energies of different commensurate structures are calculated within the mean-field approximation, by a straightforward iteration procedure, and the results are compared with each other in order to identify the most stable structure.

The mean-field model presented above accounts for a great part of the observed properties of $\text{ErNi}_2\text{B}_2\text{C}$. Figure 2 shows the magnetization curves calculated at 2 K in comparison with the experimental results. All the calculated results are based on commensurate structures derived from the basic structure at $Q = \frac{1}{2}$. At low temperatures the moments have an averaged magnitude of about $7.9\mu_B$ and in one ferromagnetic layer they are either pointing parallel (u) or antiparallel (d) to the b axis ($\mathbf{Q} \parallel \mathbf{a}$). In the $Q = \frac{1}{2}$ structure the ferromagnetic layers perpendicular to the a axis are polarized subsequently $uudduudd \dots$ along the a direction.

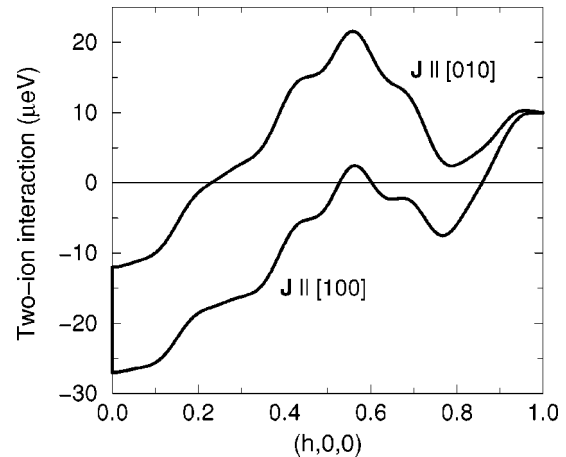


FIG. 1. The perpendicular and parallel components of the two-ion interaction in $\text{ErNi}_2\text{B}_2\text{C}$ along $[100]$.

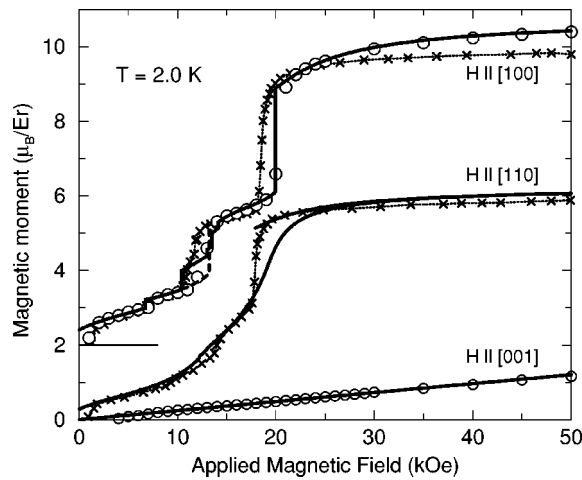


FIG. 2. The magnetization curves of $\text{ErNi}_2\text{B}_2\text{C}$ at 2 K. The open circles are the experimental results of Cho *et al.*¹⁴ The crosses connected by dashed lines show the experimental results of Canfield *et al.*² The remaining solid and dashed lines are the calculated results. The experimental and theoretical results in the case of $H \parallel [100]$ have been shifted upwards by 2 units.

Structures with larger values of Q are derived from this structure by a periodic replacement of one or more of the $uu(dd)$ double layers with a single $u(d)$ layer, the so-called spin-slip structures.¹⁵ Important structures in the present case are the $Q = \frac{6}{11}$ structure consisting of the eleven layered period $d(uudd)^2uu = d(5p)$, the eighteen layered $Q = \frac{5}{9}$ structure with the period $d(uudd)^2u(dduu)^2 = d(4p)u(4p)$, and the seven layered $Q = \frac{4}{7}$ structure with the period $duudduu = d(3p)$. Experimentally, the length of the ordering wave vector lies in the interval between 0.554 and 0.548,⁴ which range is covered by appropriate combinations of the three genetic structures. If the moments are of constant length, the $d(5p)$ and the $d(3p)$ structures have a net ferromagnetic component equal to $\frac{1}{11}\mu_{\text{max}}$ and $\frac{1}{7}\mu_{\text{max}}$, respectively, whereas the structure $d(4p)u(4p)$ has no uniform component.

If the fundamental harmonic is the only one present the free energy has its minimum value at the wave vector at which the two-ion coupling has its maximum, i.e., at $Q_0 = 0.558$ in the mean-field model. However, the intensities of the higher-order odd harmonics increase as the temperature is lowered, which produces a shift of the ordering wave vector to a smaller value. In the model $Q = 0.558$ at T_N , it decreases rapidly between 5 and 3 K to become about 0.55 below 3 K. This behavior is consistent with the experimental observation⁴ of a change of the ordering wave vector between 5 and 3 K from 0.554 to 0.548. In the neutron-diffraction experiment of Choi *et al.*⁴ the peak due to the fundamental harmonic is found to be centered at $Q = 0.548$ at 2.4 K, however the higher harmonics indicate that the main part of the crystal is actually ordered in a commensurate structure with $Q = \frac{11}{20} = 0.55$. At 2.4 K, the stable structure with this wave vector is the 40-layered structure $d(4p)u(5p)u(4p)d(5p)$. This structure, like the $d(4p)u(4p)$ structure above, has no ferromagnetic component. However, due to the increasing importance of the

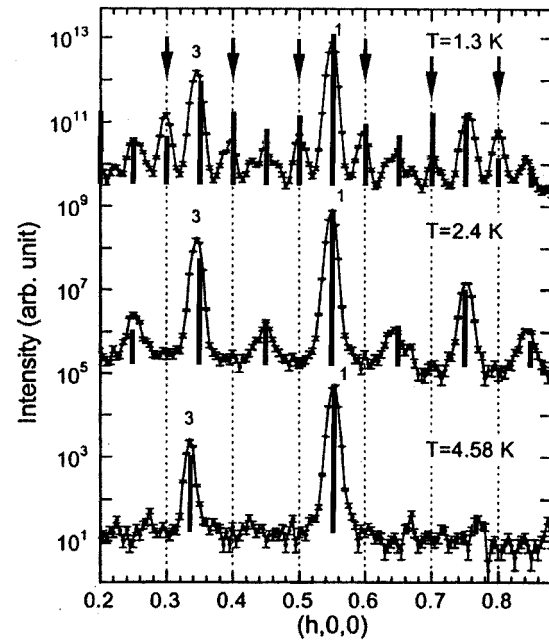


FIG. 3. Scan along $[h,0,0]$ at $T = 1.3$ K, 2.4 K, and 4.38 K, measured with unpolarized neutrons. The data have been offset for clarity. The figure is a copy of Fig. 1 from Ref. 4 in which the calculated diffraction patterns in the different cases (the heavy solid lines) have been incorporated.

higher harmonics as the temperature is lowered these structures are found to become unstable. The present mean-field model predicts the occurrence of the first-order transition

$$d(4p)u(5p)u(4p)d(5p) \rightarrow d(3p)d(5p)d(5p)d(5p) \quad (5)$$

at 2.24 K. Numbering the layers from left to right by 1 to 40, then the transition is accomplished by a reversal of the moments in the layers 9 and 20. The length of the moments changes slightly from one layer to the next, and the ferromagnetic moment is calculated to be $0.33\mu_B/\text{Er}$ just below the transition, and to be 0.40, 0.56, and $0.62\mu_B/\text{Er}$ at 2, 1.3, and 0 K, respectively, in agreement with the experimental values^{2,4} of $0.33\mu_B/\text{Er}$ at 2 K and $0.57\mu_B/\text{Er}$ at 1.3 K. The diffraction patterns of the different structures have been calculated and are compared with the results of the neutron-diffraction experiment of Choi *et al.*⁴ in Fig. 3. At 1.3 K the $d(3p)d(5p)d(5p)d(5p)$ configuration gives rise to both odd and even harmonics (the even ones are marked by arrows), twice as many as produced by the $d(4p)u(5p)u(4p)d(5p)$ structure at 2.4 K. The only discrepancy of some importance is the large value calculated for the intensity at $h = 0.7$ at 1.3 K. The splitting of the peaks around $h = 0.45$ and 0.65 at 1.3 K may be explained if a minor part of the crystal is ordered in the $Q = \frac{28}{51}$ structure $d(3p)d(5p)d(5p)d(5p)d(5p)$. Notice, that even this small change of the fundamental Q (from 0.55 to 0.549) leads to easily observable modifications in the positions of the higher harmonics. Hence, the overall agreement between the observed and calculated positions of the higher harmonics indicates with a high degree of credibility that the main part of

the crystal is a $Q = \frac{11}{20}$ structure at 1.3 and 2.4 K. There exist other choices for the low-temperature structure with $Q = \frac{11}{20}$ than the one proposed in Eq. (5), but this structure, which is calculated to be the most stable one, is the only one producing a diffraction pattern reasonably similar to the one observed at 1.3 K.

The model calculations indicate that $\mathcal{J}(\mathbf{q})$ has a sharp peak at $\mathbf{q} = \mathbf{Q}_0$, as constructed in terms of the parameter $\mathcal{J}(\text{LD})$. If this parameter is neglected the calculated variation of Q with temperature, or as a function of field, increases drastically in disagreement with the experiments. In the present model all the structures between $Q = \frac{6}{11}$ and $\frac{5}{9}$ are so close in free energy below 3 K that the model needs to be modified in order to differentiate clearly between the different Q values in this interval. This indicates that the peak in $\mathcal{J}(\mathbf{q})$ is possibly even more pronounced than assumed in the present calculations. A strong peak in the RKKY interaction may be produced by the nesting between different areas on the Fermi surface discussed by Dugdale *et al.*,¹⁶ a nesting

which is probably also responsible for the superconducting properties of these compounds.

It is important to realize that the ferromagnetic transition in $\text{ErNi}_2\text{B}_2\text{C}$ is not due to a ferromagnetic interaction, one which is actually strongly negative. The ferromagnetic component is a byproduct of the low-temperature commensurable structure. Even a large change of $\mathcal{J}(\mathbf{0})$ only has a slight influence on the transition, as the exchange-energy gain of this phase relative to the pure antiferromagnetic phase is determined by the combined contribution of all the even harmonics. This means that the influence of the superconducting electrons on this transition, as for instance through the Anderson–Suhl mechanism,^{7,8} is weak. The model is going to be examined more closely in a paper presenting a neutron-diffraction determination of the magnetic structures in an applied field.¹⁷

Valuable discussions with P. Hedegård, K. Nørgaard Toft, and N. H. Andersen are gratefully acknowledged.

-
- ¹J.W. Lynn, S. Skanthakumar, Q. Huang, S.K. Sinha, Z. Hossain, L.C. Gupta, R. Nagarajan, and C. Godart, *Phys. Rev. B* **55**, 6584 (1997).
- ²P.C. Canfield, S.L. Bud'ko, and B.K. Cho, *Physica C* **262**, 249 (1996).
- ³H. Kawano, H. Takeya, H. Yoshizawa, and K. Kadowaki, *J. Phys. Chem. Solids* **60**, 1053 (1999).
- ⁴S.-M. Choi, J.W. Lynn, D. Lopez, P.L. Gammel, P.C. Canfield, and S.L. Bud'ko, *Phys. Rev. Lett.* **87**, 107001 (2001).
- ⁵H. Kawano-Furukawa, H. Takeshita, M. Ochiai, T. Nagata, H. Yoshizawa, N. Furukawa, H. Takeya, and K. Kadowaki (unpublished).
- ⁶A. Amici, P. Thalmeier, and P. Fulde, *Phys. Rev. Lett.* **84**, 1800 (2000).
- ⁷K. Nørgaard, M.R. Eskildsen, N.H. Andersen, J. Jensen, P. Hedegård, S.N. Klausen, and P.C. Canfield, *Phys. Rev. Lett.* **84**, 4982 (2000).
- ⁸P.W. Anderson and H. Suhl, *Phys. Rev.* **116**, 898 (1959).
- ⁹U. Gasser, P. Allenspach, F. Fauth, W. Henggeler, J. Mesot, A. Furrer, S. Rosenkranz, P. Vorderwisch, and M. Buchgeister, *Z. Phys. B: Condens. Matter* **101**, 345 (1996).
- ¹⁰C. Detlefs, A.H.M.Z. Islam, T. Gu, A.I. Goldman, C. Stassis, P.C. Canfield, J.P. Hill, and T. Vogt, *Phys. Rev. B* **56**, 7843 (1997); C. Detlefs, D.L. Abernathy, G. Grübel, and P.C. Canfield, *Europhys. Lett.* **47**, 352 (1999).
- ¹¹J. Jensen and A. R. Mackintosh, *Rare Earth Magnetism: Structures and Excitations* (Oxford University Press, Oxford, 1991).
- ¹²R.A. Cowley and J. Jensen, *J. Phys.: Condens. Matter* **4**, 9673 (1992).
- ¹³J. Jensen, *Phys. Rev. B* **54**, 4021 (1996).
- ¹⁴B.K. Cho, P.C. Canfield, L.L. Miller, D.C. Johnston, W.P. Beyermann, and A. Yatskar, *Phys. Rev. B* **52**, 3684 (1995).
- ¹⁵D. Gibbs, D.E. Moncton, K.L. D'Amico, J. Bohr, and B.H. Grier, *Phys. Rev. Lett.* **55**, 234 (1985).
- ¹⁶S.B. Dugdale, M.A. Alam, I. Wilkinson, R.J. Hughes, I.R. Fisher, P.C. Canfield, T. Jarlborg, and G. Santi, *Phys. Rev. Lett.* **83**, 4824 (1999).
- ¹⁷K. Nørgaard Toft *et al.* (unpublished).